

## Morphology of nightside precipitation

Patrick T. Newell,<sup>1</sup> Yasha I. Feldstein,<sup>2</sup> Yuri I. Galperin,<sup>3</sup> and Ching-I. Meng<sup>1</sup>

**Abstract.** Considerable information on the state of the magnetosphere is embedded in the structure of nightside charged particle precipitation. To reduce ambiguity and maximize the geophysically significant information extracted, a detailed scheme for quantitatively classifying nightside precipitation is introduced. The proposed system, which includes operational definitions and which has been automated, consists of boundary 1, the “zero-energy” convection boundary (often the plasmopause); boundary 2e, the point where the large-scale gradient  $dE/d\lambda$  switches from positive to  $\leq 0$  (the start of the main plasma sheet); boundary 2i, the ion high-energy precipitation cutoff (the ion isotropy boundary or the start of the tail current sheet); boundaries 3a,b, the most equatorward and poleward electron acceleration events (spectra with “monoenergetic peaks”) above  $0.25 \text{ erg/cm}^2 \text{ s}$ ; boundary 4s, the transition of electron precipitation from unstructured on a  $\geq 10\text{-km}$  spatial scale (spectra have 0.6–0.95 correlation coefficients with neighbors) to structured (correlation coefficient usually 0.4 and below); boundary 5, the poleward edge of the main auroral oval, marked by a spatially sharp drop in energy fluxes by a factor of at least 4 to levels below those typical of the auroral oval; and boundary 6, the poleward edge of the subvisual drizzle often observed poleward of the auroral oval.

### 1. Introduction and Background

Thirty years ago the first precipitation classification scheme was introduced: *Johnson et al.* [1966] identified a hard zone and a soft zone, the latter defined by the presence of counts in the  $>80\text{-eV}$  electron detector but not in the  $>21\text{-keV}$  detector. This classification system had an elegant simplicity and operational clarity not subsequently approached. It lacked only utility and geophysical significance. *Burch* [1968] showed that the soft zone existed on both the dayside and nightside but was softer on the former. Later it was shown that some of the dayside precipitation originates in the magnetosheath [*Heikkila and Winningham*, 1971; *Frank*, 1971]. In a series of papers we have previously discussed the classification and quantitative identification of various types of dayside precipitation [*Newell and Meng*, 1988a; *Newell et al.*, 1991a, b; cf. *Cambou and Galperin*, 1974; *Sauvaud et al.*, 1980; *Galperin et al.*, 1976].

Twenty years ago *Winningham et al.* [1975] (hereafter referred to as WYAH75) made a major advance in describing the nightside precipitation morphology and its dependence on the substorm cycle. They divided the precipitation into plasma mapping to the near-Earth quasi-dipolar field lines, which they referred to as “the central part of the plasma sheet” and hence termed the CPS, and plasma

originating from the more stretched field line region where most electron acceleration events occur. This latter they termed the “boundary plasma sheet” (BPS). WYAH75 did not give clear operational definitions for identifying their CPS and BPS precipitation regions, choosing to illustrate with examples. This has led to a certain ambiguity in terminology which further complicates a discussion of physics questions. For example, various interpretations of the poleward boundary of “Winningham’s CPS” exist in the literature, including the start of structured satellite auroral imagery [*Lui et al.*, 1977], the onset of highly structured electron precipitation [*Newell et al.*, 1991c], and the stable trapping boundary of  $>35\text{-keV}$  electrons [*Deehr et al.*, 1976; *Weiss et al.*, 1992].

WYAH75 associated the CPS with diffuse aurora, as defined by *Lui and Anger* [1973], and the BPS with discrete aurora. They reported that the CPS was relatively unchanged by the substorm cycle but that the BPS in quiet times had a deactivated phase in which only soft electron precipitation was observed as well as an activated (substorm) phase in which the BPS was energized. Later the view that the BPS was associated with the high-altitude plasma sheet boundary layer (PSBL) signature became common. For example, *Eastman et al.* [1984, p. 1554] state that the BPS is the “probable low-altitude signature of the [high-altitude] plasma sheet boundary layer” (see also *Rostoker and Eastman* [1987]).

*Feldstein and Galperin* [1985] (hereinafter referred to as FG85) argued against this interpretation for several reasons. Some of their objections, when well understood, prove to be primarily issues of terminology. For example, FG85 did not believe that the region of hot plasma on quasi-dipolar field lines earthward of the tail current sheet should be termed the “central plasma sheet”; indeed, they argued that this term should apply only to the plasma that lies tailward of the earthward edge of the current sheet. The apparent conflict between FG85 and WYAH75 was worsened because of the operational ambiguity in defining

<sup>1</sup>The Johns Hopkins University Applied Physics Laboratory, Laurel, Maryland.

<sup>2</sup>Ionosphere and Radiowave Propagation, Institute of Terrestrial Magnetism, Troitsk, Russia.

<sup>3</sup>Institute of Space Research of the Academy of Sciences of Russia, Moscow.

the CPS. However, even beyond all these (and other) issues of terminology, FG85 had an unassailable argument in that the region identified as PSBL at high-altitude was only a tiny fraction of the full plasma sheet thickness; yet the low-altitude BPS could well constitute the majority of the auroral oval width. The arguments of FG85, further advanced in *Galperin and Feldstein* [1991] with a discussion of recently discovered phenomena such as velocity-dispersed ion signatures (VDIS-2), made clear to all who studied the issue that in fact the PSBL does not map to the entire low-altitude BPS. Instead, as originally proposed by *Feldstein and Starkov* [1970] and confirmed by many others [*Deehr et al.*, 1976; *Weiss et al.*, 1992], discrete auroral arcs map to the main plasma sheet which lies poleward (tailward) of the stable trapping boundary of 35-keV electrons. FG85 also pointed out that an auroral classification scheme must include an additional precipitation region, namely, subvisual drizzle which lies poleward of the main auroral oval. They cited a long but little noted history of measurements requiring such a separate classification (e.g., *Eather* [1969]).

In the present paper we revisit the question of nightside morphology for three reasons: (1) Much new research has been done in recent years on the phenomenology of nightside precipitation. This research makes it possible to introduce a nightside classification system with more geophysically significant information. (2) Because it has recently become obvious that researchers use the same terms in quite different ways, we wish to introduce operationally unambiguous algorithms for identifying these significant boundaries. (3) The phenomenology of nightside precipitation is more complex than reported by WYAH75, and, in some instances, their discussion requires modification. Notably neither the CPS, however defined, nor any other precipitation region is substantially independent of substorm cycle. Indeed, the CPS of WYAH75 almost disappears after ~16 hours of extreme magnetic quiet.

The data presented herein are from the Defense Meteorological Satellite Program (DMSP) F7 polar-orbiting satellite, which was in a nearly circular 835-km-altitude orbit with 98.7° inclination. F7 was Sun synchronous, lying in the 1030–2230 magnetic local time (MLT) plane. The SSJ4 particle detectors onboard measured electrons and ions from 32 eV to 30 keV in 19-point spectra with 1-s resolution [*Hardy et al.*, 1984]. The satellite was three-axis stabilized, with the SSJ4 aperture always pointed toward zenith so that at auroral latitudes only particles well within the loss cone were sampled.

## 2. Structure of Nightside Precipitation: Physical Significance of the Boundaries

As in many situations, an example is clearer than words alone; hence consider Plate 1, which presents a DMSP F7 pass at 1123 UT on January 3, 1985 during a recovery phase. Plate 1 is presented as a typical case; a discussion of the effects of substorm cycle is deferred until section 4. We consider in turn each of the most geophysically significant boundaries that can be identified in this picture. Because operational definitions which are robust require an attention to detail that is tedious to many, section 2 gives conceptually oriented definitions, with the fine print reserved for section 3.

**Boundary 1, the zero-energy convection boundary** (1127:13 UT). Zero-energy electrons and ions have no curvature or gradient drifts, hence they should share a common equatorward boundary, one which is determined purely by the electric and magnetic field configuration (that is, the boundary which results only from a consideration of  $\mathbf{ExB}$  drift effects). The DMSP low-energy ion detector has an extremely large geometric factor, which makes it possible to observe such coincidences despite the comparatively low fluxes of ions at low energies. *Newell and Meng* [1988b] have reported that in the dusk and midnight sectors the electron and ion zero-energy cutoffs indeed coincide on 80% of the passes. To maintain operational unambiguity, we propose that the zero-energy electron and ion boundaries be separately defined (denoted b1e and b1i, respectively). Then, when the two boundaries indeed coincide to within 0.25° magnetic latitude, one may reasonably say that a zero-energy convection boundary exists. Any model electric or magnetic field of the magnetotail specifies a unique position for this boundary (as a function of MLT); hence observation of the boundary provides a direct comparison between theory and reality. In some theoretical formulations the zero-energy convection boundary is also the plasmopause location [*Nishida*, 1966], and, indeed, observations of electron data support this association [*Galperin et al.*, 1977; *Jorjio et al.*, 1978; *Horwitz et al.*, 1986; *Sauvaud et al.*, 1983]. However, the zero-energy boundary observed at any given time does not necessarily represent a steady-state convection boundary, since magnetotail convection is highly dynamic [*Mauk and Meng*, 1983; *Galperin et al.*, 1975]. Indeed, the low-energy equatorward ion precipitation often contains plasma originally of ionospheric origin, apparently injected at high latitudes often in association with auroral arcs [*Jorjio et al.*, 1985; *Bosqued et al.*, 1986; *Cambou and Galperin*, 1974, 1982]. However, its subsequent convection toward lower latitudes is the result of  $\mathbf{ExB}$  drift effects. To maintain operational unambiguity, and because the zero-energy boundary has theoretical importance in its own right, we do not stress here the connection with the plasmopause.

**Boundary 2e, the poleward edge of the  $dE_e/d\lambda > 0$  region** (1125:47 UT). It has long been known that low-energy electrons in the plasma sheet reach closer to Earth than do higher-energy electrons [*Vasyliunas*, 1968; *Schield and Frank*, 1970; *Fairfield and Vinas*, 1984]. The higher the energy of the electrons measured, the farther from the Earth they appear to have a cutoff (some exceptions exist, such as when a dispersionless injection occurs). As a low-altitude spacecraft moves poleward from boundary 1e, progressively higher-energy electrons are observed, so that  $dE_e/d\lambda > 0$  (where  $E_e$  is the average energy of the electrons). As one reaches the main plasma sheet, electrons of all energies are observed. Farther poleward the overall trend is for  $dE_e/d\lambda < 0$  (the region of negative gradient has a slope of smaller magnitude and exhibits more fluctuations than does the region of positive gradient), simply because the plasma sheet is progressively colder farther from the Earth. The point where  $dE_e/d\lambda = 0$  is one measure of the start of the main plasma sheet (or in the terminology of FG85, the true start of the central plasma sheet).

**Boundary 2i, the high-energy ion equatorward precipitation cutoff or precipitating energy flux maximum** (1126:00 UT). This boundary is also the isotropy boundary

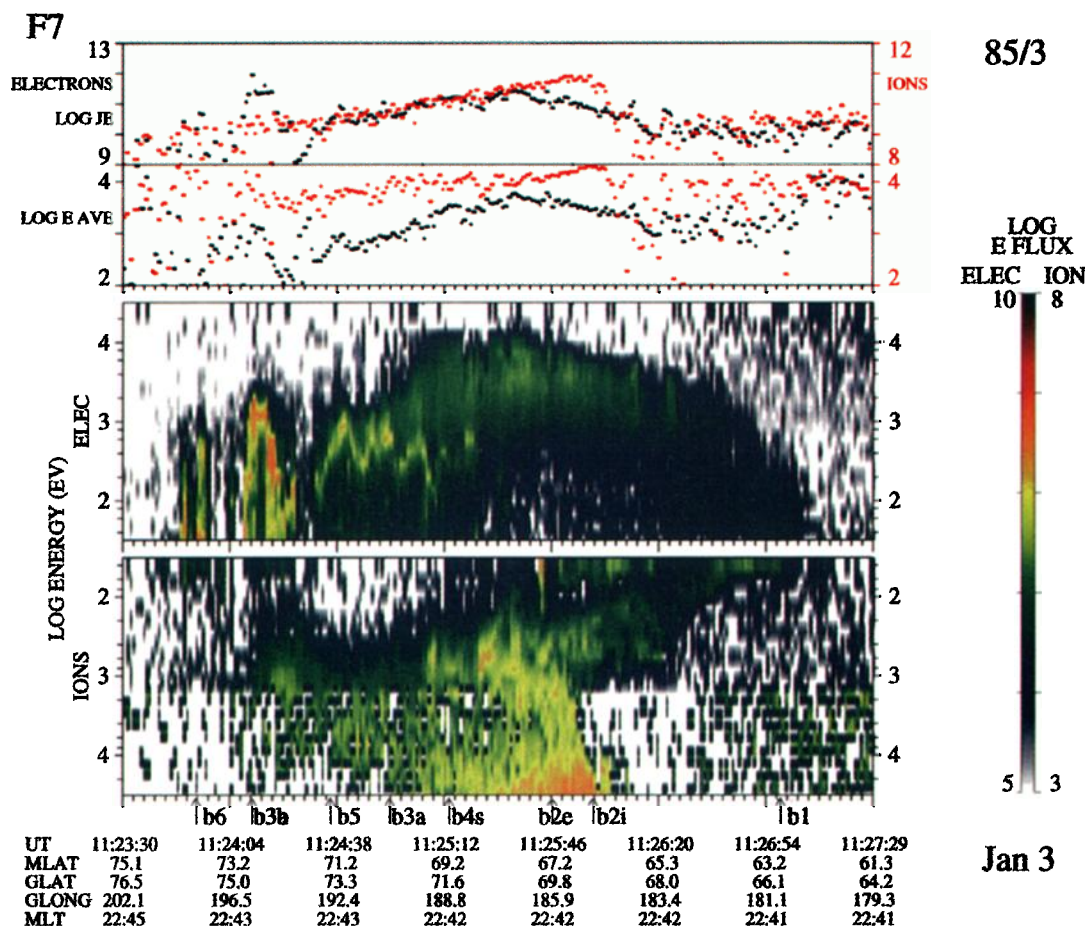


**Plate 1.** A typical precipitation pattern observed in crossing the nightside auroral oval by DMSP F7 on January 3, 1985 at 1123 UT. Plotted are differential energy fluxes in units of  $\text{eV}/\text{cm}^2 \text{ s sr}$   $\text{eV}$  (main panels); average energy in  $\text{eV}$  (bottom plot), and integral energy flux in  $\text{eV}/\text{cm}^2 \text{ s sr}$ .

(IB) of *Sergeev et al.* [1983]. It is probably the best and most direct proxy for the location of the earthward edge of the current sheet. Consider ions in the energy range from a few keV to tens of keV (30 keV for DMSP). Ions in this energy range increase in temperature and energy flux with declining latitude, apparently as a result of adiabatic acceleration as plasma convects earthward in the magnetotail [*Galperin et al.*, 1978]. This steady temperature increase terminates with a relatively sharp equatorward precipitation cutoff. However, in the high-altitude inner magnetosphere, ions do not disappear at the L-shell value of the high-energy ion precipitation boundary (e.g., *Lui et al.* (1987)). Instead, the ions become trapped and cease to precipitate in measurable quantities. Poleward of the precipitation boundary at any particular energy, the ions are highly isotropic [*Bernstein et al.*, 1974; *Sergeev et al.*, 1993]. It has thus been suggested, and even successfully modeled in some detail, that the ions maintain their isotropy by pitch angle scattering in the tail current sheet [*Lyons and Speiser*, 1982]. The physical mechanism is quite simple: ions cannot maintain pitch angle while bending around field lines that have a radius of curvature comparable to the ion gyroradius [*Sergeev et al.*, 1983]. This explanation also accounts for the dispersion in the high-energy ion cutoffs [*Sergeev et al.*, 1993]. The larger gyroradii of higher-

energy ions means that they scatter off field lines with smaller radii of curvature than do the lower-energy ions; hence the higher-energy ions maintain isotropy farther earthward.

Neither the tail current sheet nor the precipitating high-energy ions have a sharply defined boundary. Operationally we propose to use the ion precipitating energy flux peak (integrated over the range 3–30 keV), which universally occurs near the equatorward boundary of the high-energy ion precipitation, as the definition of b2i. The geophysical significance of the boundary is that it represents a good approximation to the earthward edge of the tail current sheet. *Sergeev and Gvozdevsky* [1995] have demonstrated that the latitude of this ion isotropy boundary has a very high correlation ( $r \sim 0.9$ ), with the magnetic field inclination (degree of stretching) measured simultaneously at the geomagnetic equator.

A conceptually closely related boundary is the >30–40-keV electron-stable trapping boundary for electrons, which we term b2t. Although we cannot directly identify it in our DMSP database, it has long been considered useful. Thought in the 1960s to represent the open/closed field line boundary, b2t is now generally recognized as another measure of where field lines begin to be significantly stretched (see the discussion on pp. 246–247, FG85). Be-

tegral parameters are denoted  $n$ ,  $j_E$ , and  $E$ , referring to density, energy flux, and average energy, respectively. These quantities can take the subscript “e” for electrons or “i” for ions. Better results are obtained if the terms  $jep(E1, E2)$  etc. are introduced, referring to the “partial” electron energy flux between  $E1$  and  $E2$ . Strictly speaking, all instruments measure only partial values of “integral” parameters between the upper and lower ranges of their detector (some confusion in the literature exists from the neglect of this point, as in the case of the cusp electron average energy). As a practical consideration here, such partials improve greatly the identification of boundaries while also making the results somewhat less dependent on the specific detector (SSJ4) that they were designed for. The units used below are eV for  $E$  and  $\log_{10} \text{ eV/cm}^2 \text{ s sr}$  for  $jep$  and  $jip$ . For each boundary, we start by giving the rule that works most of the time and follow with caveats and more detail on handling special cases.

**Boundaries b1e,i (zero-energy).** The algorithm moves from lower latitudes to higher, comparing the average of  $jip(E1, E2)$  and  $jep(E1, E2)$  (ordinarily  $E1$  and  $E2$  are the two lowest channels) over the three previous spectra with the three succeeding spectra. An increase in  $jip$  by a factor of 2 marks the onset of the zero-energy boundary, which is separately determined for the two species. This jump is

significant only if it also significantly exceeds the background counts obtained by averaging over several equatorward seconds. If  $jep$  rises to a value above 8.0 (or if  $jip$  reaches 6.5), a factor of only 1.6 jump is acceptable in determining the zero-energy boundary. If  $jep > 8.25$  ( $jip > 6.9$ ), it is assumed that the boundary has been reached, even if no jump in the value of the fluxes is measured.

**Special cases:** The energy range considered ( $E1$  to  $E2$ ) in the partials depends on whether photoelectrons are present and whether the spacecraft is charged to  $-28 \text{ V}$ . The former can be identified by a sharp drop-off in electron fluxes above 68 eV at latitudes below the auroral zone, the latter by a sharp cutoff above the 32-eV ion channel. In the absence of these effects the channels are set to the lowest available value, i.e.,  $E1 = 32$  and  $E2 = 47$ . If the spacecraft is charged to  $-28 \text{ V}$ , the ion channels are set to  $E1 = 47$  and  $E2 = 68$ . If photoelectrons are present (rare on the nightside), the next available “clean” channels are 100 and 145 eV, respectively. Finally, isolated noise can sometimes cause false positives, as by radiation belt counts at 1118:30 UT in Plate 4. Thus a “check b1e” routine performs a double-check by simply examining the next several seconds. If, in the next few seconds as the auroral oval is purportedly entered, a drop-

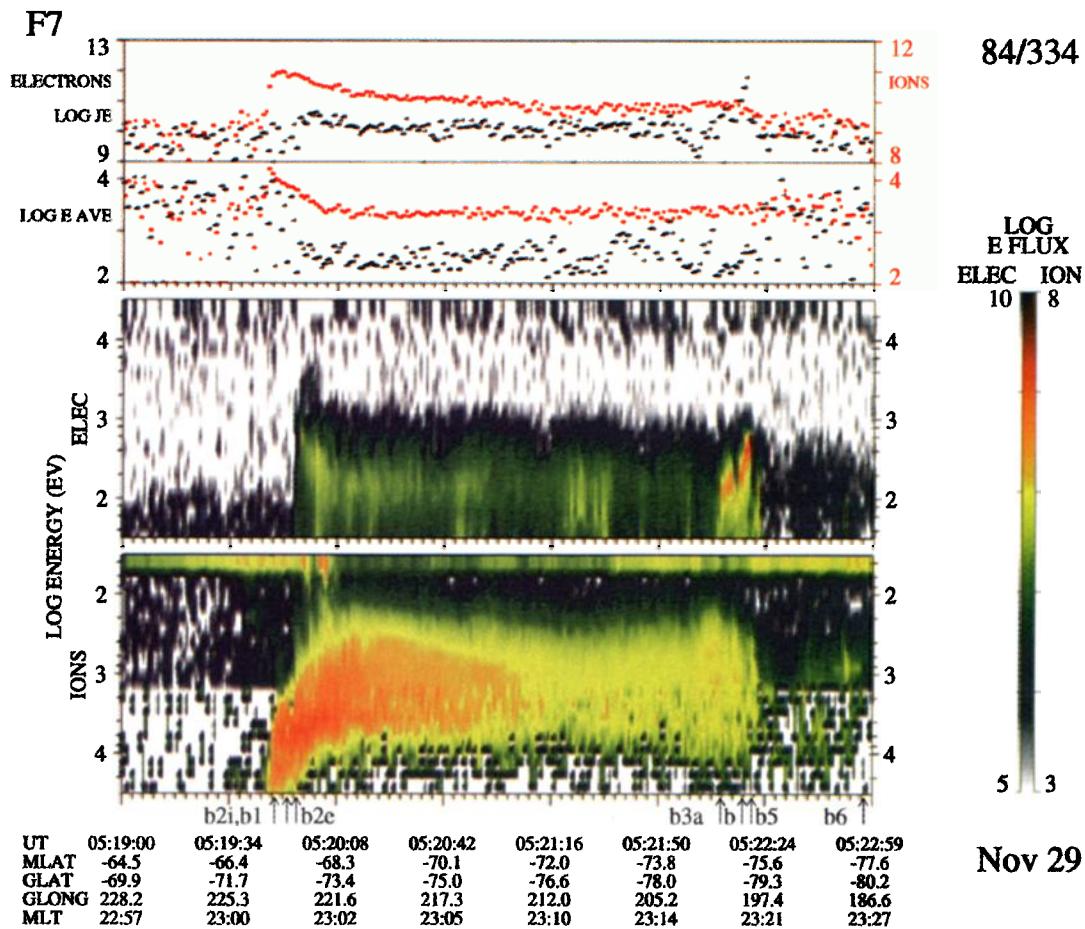


Plate 2. The nightside auroral oval under conditions of prolonged quiet (November 29, 1984 at 0519 UT).

off in fluxes is exhibited instead of a rise in fluxes, the identification of b1e is inaccurate, and the search resumes toward increasing latitudes.

**Boundary b2e (plasma sheet start).** This algorithm locates the first point poleward of b1e where  $dE_e/d\lambda \leq 0$ . A sliding 3-s average  $E_e$  is compared to that of any 3 consecutive seconds over the next 9 s. If the value of  $E_e$  does not rise over this interval, the boundary b2e has been located.

**Special cases:** If the correct boundary b2e has been found, one expects to have entered the main plasma sheet. Hence if  $j_{E_e} < 11$  (or if both  $j_{E_e} < 11.5$  and  $E_e < 1000$  eV), then the next 30 s are examined to see if a spectrum exists with a higher  $E_e$  as well as a  $j_{E_e}$  larger by at least 0.3 (i.e., a factor of 2 difference in the energy flux). Double checking is done only under this suspicious circumstance of low fluxes because it risks encountering a point with high  $E_e$  and high  $j_{E_e}$  simply because strong field-aligned acceleration is encountered.

**Boundary b2i (ion isotropy boundary).** This boundary is defined by the precipitation flux maxima for ions 3 keV and above. The high-energy ions behave less variably than do the electrons, so fewer precautions are needed. Thus a sliding average of  $j_{ip}(3 \text{ keV}, 30 \text{ keV})$  over 2 s is compared with  $j_{ip}$  for any 3 consecutive seconds over the next 10 s farther poleward to determine whether the maximum has been located. The smallest maximum acceptable is 10.5.

**Special cases:** Sometimes "nose" events occur, namely, the injection of high-energy ion regions slightly detached from the rest of the auroral oval [Konradi et al., 1975; Sánchez et al., 1993]. Such events are identified as local maxima followed by a decline and subsequent rise to global energy flux maxima. The detached (or partially detached) maximum is discarded. In addition, in times of prolonged quiet, b2i may occur equatorward of b1i (as in Plate 2), but by definition b2e must always lie poleward of b1e.

**Boundaries b3a,b (most equatorward and poleward electron acceleration events).** Each individual spectrum is examined for evidence of a monoenergetic peak. This can either be a single channel with a differential energy flux 5 times larger than any other or a sharp drop by at least a factor of 10 below the electron differential energy flux peak. Details of this algorithm, including special cases, are presented in a separate paper [Newell et al., 1996]. The most equatorward and poleward individual spectra showing such monoenergetic peaks are flagged as boundaries b3a and b3b, without regard to other boundary locations.

**Boundary b4s (structured/unstructured boundary).** The counts in the various channels for a given spectrum are correlated with the corresponding counts in the five previous spectra, and the five resulting correlation coefficients are averaged ( $\langle r \rangle$ ). By definition b4s lies poleward of b2e and b2i. When the sum of seven consecutive  $\langle r \rangle$

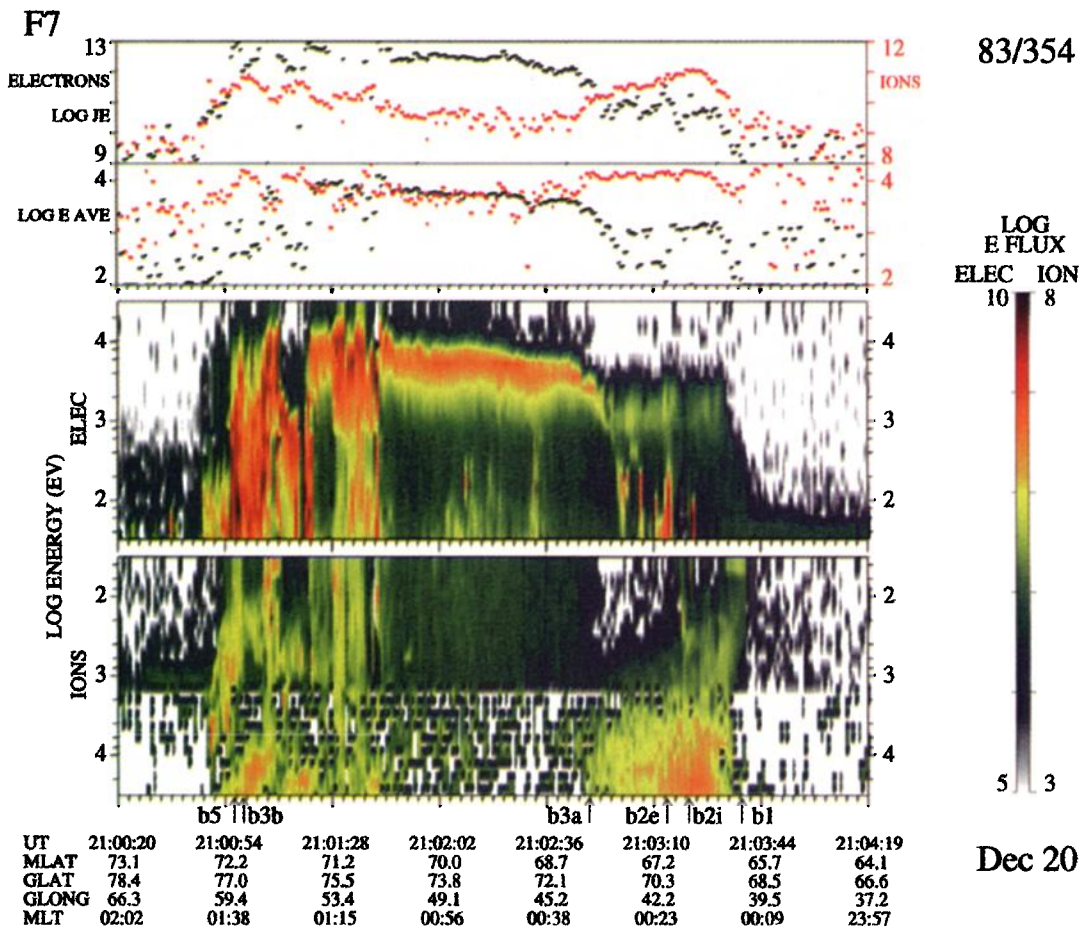


**Plate 3.** The nightside precipitation pattern shortly after an onset which followed a period of prolonged quiet (December 20, 1983 at 2100 UT).

drops below 4.0, the search is halted. b4s is set to be the farthest poleward spectrum within the final group of 7 s, which has  $\langle \gamma \rangle > 0.60$ .

Special case: If the energy fluxes result only in an aurora which is subvisual ( $j_e < 10.7$  or  $0.25 \text{ erg/cm}^2 \text{ s}$ ), the correlation coefficient is suppressed (halved); hence low-flux but homogeneous regions such as polar rain are automatically excluded.

**Boundaries b5e,b5i (poleward edge of main oval).** These boundaries are computed separately, but using the same procedure. An average of  $j_E$  for the previous 12 s is compared with  $j_E$  for the succeeding 12 s. When a drop-off of a factor of 4 is located, a provisional b5 boundary is determined. Note that this algorithm emphasizes locating a sharp gradient in the flux levels.

Special cases: The next 30 s are double-checked (35 s for electrons) to make sure the drop-off remains below auroral energy fluxes. If the (log) average  $j_E$  has not dropped below about 9.7 for ions or 10.5 for electrons, the search continues for the corresponding b5 boundary. Such a large search ahead is needed because of features like the "double oval" [Elphinstone et al., 1995] in which fluxes cause of the smaller gyroradii of electrons, b2t usually lies a short distance poleward of b2i. There is some reason to believe that the stable trapping boundary approximately corresponds to the WYAH75 boundary between CPS and BPS; and, indeed, Weiss et al. [1992] define this latter

boundary by the trapping boundary. Auroral arcs apparently invariably occur poleward of b2i (cf. Lyons et al. [1988]).

**Boundaries 3a,b, the most equatorward and poleward electron acceleration events.** In the literature many proxies for identifying the region of discrete auroras exist. For example it appears that most electron acceleration events, and certainly those of high accelerating potential values, occur on the stretched field lines that lie poleward of the  $>40\text{-keV}$  electron-stable trapping boundary [Frank and Ackerson, 1971]. It is quite feasible to examine each electron spectrum and determine whether it shows signs of a field-aligned accelerating potential. Therefore we include boundaries 3a and 3b, which, based on the examination of each individual spectrum, are the farthest equatorward and farthest poleward sites of electron acceleration. A spectrum is identified as accelerated if it has either a monoenergetic peak or a sharp cutoff above the spectral peak (more detail is available in Newell et al. [1996]). Although we have opinions about the likely location of these boundaries, it is best that they be identified separately from all other precipitation boundaries.

**Boundary 4s, the onset of spatial structure in electron precipitation (on a scale of  $\geq 5\text{--}10 \text{ km}$ ) (1125:14).** The BPS/CPS distinction, no matter what misconceptions became associated with it, has persisted primarily because many nightside crossings do seem to have a highly struc-

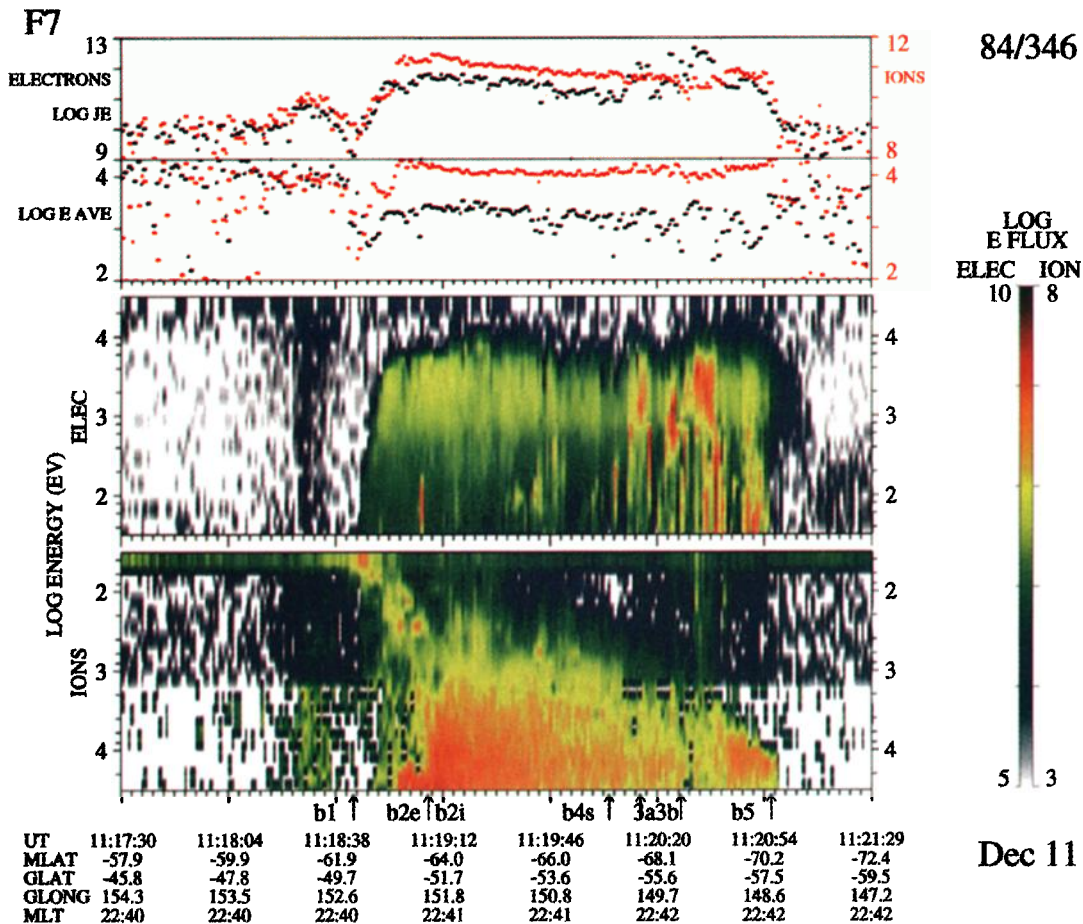


**Plate 4.** The nightside auroral oval during conditions of moderate activity (December 11, 1984 at 1117 UT).

tured region as well as a relatively unstructured region of auroral electron precipitation. If this structured/unstructured distinction represents something fundamental, there should be a quantitative way of making the distinction within the precipitation data themselves, i.e., one that does not depend on such additional factors as the boundary of the radiation belts (b2t).

To move from a qualitative description (structured) to a quantitative description, we investigated the behavior of the correlation coefficient of individual spectra with their neighbors. Figure 1 shows a plot of the running average of the correlation coefficient of each spectrum in Plate 1 with the previous five spectra. (Our algorithm suppresses spectra with fluxes below  $0.25 \text{ erg/cm}^2 \text{ s}$  by halving the correlation coefficient.) Although even within the BPS region most of the individual spectra do not show evidence of field-aligned acceleration, Figure 1 shows that the entire region is indeed structured in the sense that each point correlates only poorly with its neighbors. We therefore introduce boundary 4s, the structured precipitation boundary, defined by the point where the correlation coefficient drops from the 0.95–0.60 range to below 0.60. Thus b4s marks a fundamental change in the character of the electron precipitation, from a spatially unstructured region to a highly structured one. Section 5 points out that some limited fine-scale structure may appear within the generally unstructured precipitation region; in this sense it is “unstructured” over spatial scales  $>5\text{--}10 \text{ km}$ .

**Boundaries 5e,i, the poleward boundaries of the main auroral oval (1124:36 UT).** The precipitating energy flux in the auroral oval typically drops by about an order of magnitude over a short distance (usually  $<0.2^\circ$ ). This dramatic drop-off occurs in both the electrons and ions, although not always in precisely the same location for the two species. In active times, poleward of this sharp drop-off, there is often only a narrow region of high-energy ( $\sim 10\text{-keV}$ ) but diffuse electrons at very low flux levels. (This faint “overhang” of high-energy electrons seems to be both unremarked in the literature and a common feature

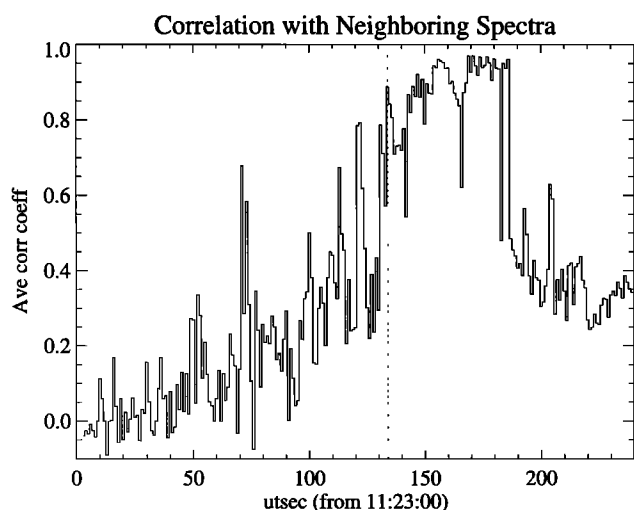


**Figure 1.** A plot of the average correlation coefficient of each electron spectrum with its five predecessors for the pass shown in Plate 1. The dashed line shows the poleward boundary of structured precipitation, b4s.

in nature.) Sometimes, especially in quiet times, including quieting times following a substorm, a subvisual drizzle can extend poleward of the oval. The conceptual definition of the poleward edge of the main auroral oval is that the precipitating fluxes drop by a factor of at least 4 over a short distance to values below  $3 \times 10^{10} \text{ eV/cm}^2 \text{ s sr}$  (electrons) or  $10^{10} \text{ eV/cm}^2 \text{ s sr}$  (ions). We emphasize that even for northward interplanetary magnetic field (IMF) conditions such sharp drop-offs still occur and separate the main auroral oval from the polar cap precipitation (which, to be sure, usually resembles the structured plasma sheet precipitation, although not at the intensity of the main oval).

**Boundary 6, the poleward boundary of the subvisual drizzle (1123:53 UT).** Poleward of the main auroral oval is a weak subvisual drizzle that differs from polar rain in several ways. The subvisual drizzle usually includes weak ion as well as electron precipitation; the drizzle is structured, whereas polar rain is comparatively homogeneous; and the typical electron energies are a bit higher than normal for polar rain. Polar rain is intense poleward of the dayside oval and declines gradually in intensity as it moves toward the nightside oval. The subvisual drizzle extends poleward from the nightside oval and terminates either when fluxes drop to background levels or (less commonly) when a smooth, coherent electron polar rain signature is encountered.

### 3. Operational Definitions of Nightside Precipitation

In this section we give the detail required to operationally define the various boundaries unambiguously. The intensities drop below oval levels only to rise again clearly to oval values.

**Boundary b6 (the poleward boundary of the subvisual drizzle).** This boundary is defined by the point where either polar rain is encountered (identified by the presence of unstructured electrons and no ions) or  $j_{E_e}$  drops below 10.4 and  $j_{E_i}$  drops below 9.6.

**Special cases:** The drizzle is defined by weak structured fluxes with ions and electrons above noise levels. By checking the computed average energy, one can infer whether noise is significant: For example if counts are randomly distributed across all channels, one would obtain  $E = 15 \text{ keV}$  for DMSP. If  $E_e < 500 \text{ eV}$ , even a flux as low as 10.0 is acceptable. A lower average energy implies that a lower minimum flux level is interpretable as physical.

### 4. Geomagnetic Activity and the Stages of Nightside Precipitation

Occasional intervals of prolonged quiet occur in which many hours elapse with no apparent auroral activity. Plate 2, a spectrogram from November 29, 1984 at 0519 UT, shows the precipitation observed during an extreme example of magnetic quiet. The last previous substorm ended some 16 hours previously, at least judged by the flat and near-zero values for  $AU$  and  $AL$  in the intervening interval. In this unusual case the entire CPS as defined by WYAH75 is below easily measurable levels—the region of hot but highly correlated electron precipitation (between b2e and b4s) has virtually disappeared. Also gone is the

$dE_e/d\lambda > 0$  region (between b1e and b2e), along with the similarly dispersed soft ion precipitation (between b1i and b2i). This latter coincidence between boundaries 1 and 2 is not highly unusual. The extended region of dispersed cutoffs disappears after only a few hours with no substorm activity [Newell and Meng, 1987; Sánchez et al., 1993]. There is good evidence that the ions observed between b1 and b2 are originally injected from the ionosphere at higher latitude (say between b4s and b5) in association with electron acceleration events and contain a large amount of  $O^+$  [Sauvaud et al., 1981; Bosqued et al., 1986]. Once introduced into the magnetosphere, the ions are  $\mathbf{ExB}$  convected earthward, and hence to lower latitudes. It is appropriate that FG85 termed the region between boundaries 1 and 2 "the remnant layer" since these equatorward ions and electrons do seem to be the remnants of magnetic activity (including the effects of earthward convection from the plasma sheet).

The extended region of soft electrons within the main auroral oval observable in Plate 2 corresponds to what WYAH75 termed the "unactivated BPS." The general profile of the plasma sheet population is more faithfully preserved in this instance than in the more typical (less quiet) situation: beyond about  $69^\circ$  magnetic latitude the ions and electrons have a temperature of about 1 keV and 200 eV, respectively, values quite appropriate to the plasma sheet for say  $10 R_e$  and beyond (e.g., Baumjohann et al. [1989]; Christon et al. [1989]). Only a few accelerated electron spectra (in this case, toward the poleward edge of the oval) are to be observed.

Generally the first change noticeable with the onset of auroral activity is the injection of hot plasma (10 keV and up for ions, several keV for electrons) into the equatorward (near-Earth) region of the auroral oval (Lassen et al. [1977] studied the relationship of such injected hot plasma to auroral phenomena as seen by all-sky cameras and ground-based magnetometers). Sometimes in the premidnight local time sector hot ions can be observed prior to the observation of hot electrons, as happened to be the case for the next DMSP pass after Plate 2.

To illustrate more of the features observed shortly after onset we present a different instance of substorm onset after a period of prolonged quiet in Plate 3, showing a DMSP F7 pass from December 20, 1983 at 2100 UT (the expansion phase). In this slightly postmidnight case it is the injection of the hot electrons in the equatorward region of the auroral oval which is more dramatic. Plate 3 shows two other noteworthy features: an auroral bulge is observable between 2101:37 and 2102:50 UT, and, farther poleward, the electrons are now in what WYAH75 termed an "activated" state. The form that an auroral bulge caused by substorm expansion takes in satellite precipitation observations is an extended interval of electron acceleration (monoenergetic peak spectra) in which the accelerating potential does not rise and fall in a "V"-shaped fashion but instead shows a relatively constant accelerating energy (cf. Lopez et al [1991]).

Poleward of the bulge feature (between 2100:45 and 2101:35 UT) lies the highly structured precipitation characteristic of the activated BPS of WYAH75. This region is highly structured in the sense that the correlation between neighboring electron spectra is low (typically in the 0.0–0.4 range). During active times this region contains elec-

trons of several keV, even in individual spectra that do not contain the classic signs of an accelerating downward potential. In general, as reported by WYAH75, only during quiet (or quieting) conditions does the structured region of precipitation (between our b4s and b5e) consist of comparatively soft plasma ( $kT_e < \sim 300$  eV,  $kT_i \sim 1$  keV) (we have added information on the ions to the description of WYAH75). Although we agree with the WYAH75 description of this phenomenon, it is not clear whether the original explanation is correct, that is, whether the disappearance of the "deactivated BPS" reflects the energization of that plasma population. The sharp poleward cutoffs to the electron and ion precipitation that often appear during substorm activity are reasonably ascribed to an open/closed field line boundary; it may therefore be that the ionosphere is no longer magnetically connected to the more distant plasma sheet population that originally supplied the soft precipitation.

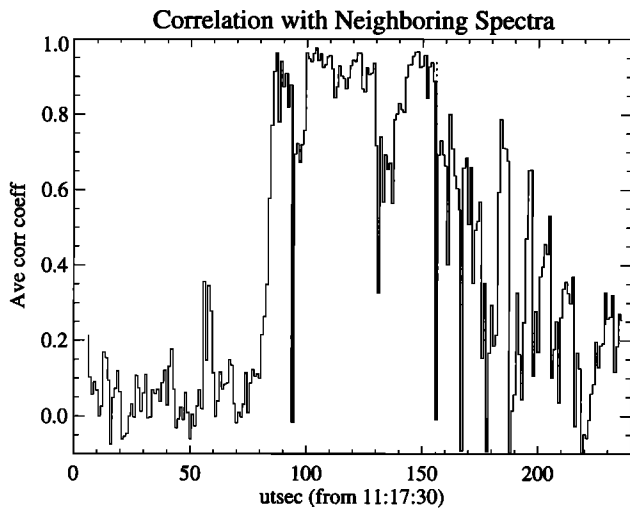
Our final example is Plate 4, representing a DMSP F7 pass from December 11, 1984 at 1117 UT, representing moderately active auroral conditions. (Note that the phenomenon observed at 1118:32 UT is caused by MeV electrons from the radiation belt penetrating the detectors and does not represent precipitation.) The  $dE_e/d\lambda > 0$  region is reasonably well developed, along with the associated low-energy ion injection. The fairly sharp poleward cutoff at 1120:58 UT is characteristic of active times and has reasonably been interpreted as representing the open/closed field line boundary. In this case one can observe at the poleward edge of the auroral oval what is a fairly common feature of active times, yet seems to be unmentioned in the literature. Notice that there is a faint high-energy ( $\sim 1$ – $15$ -keV) electron "overhang" present. Reports in the literature generally describe the poleward subvisual "polar diffuse aurora" as owing to low-energy electrons, which they often surely do. However, in the course of creating automated boundary identifications for the nightside oval, we found that this narrow and diffuse high-energy electron overhang is frequent during active times.

Figure 2 shows that the correlation coefficient allows for a rigorous separation between the structured and unstructured portions of the auroral oval. Prior to 1120:06 UT each spectrum correlated with its five preceding neighbors on the level of 0.6–0.98, albeit with occasional dips. Poleward of 1120:06 UT the correlation dropped dramatically, to the range generally below 0.5, although with occasional spikes above that level.

It remains to discuss precipitation patterns under quieting conditions following a substorm. Actually Plate 1 represents such a case. The extended  $dE_e/d\lambda > 0$  region is proof that substorm activity recently occurred, whereas the lack of energization in the poleward region of the structured auroral oval occurs only under quieting conditions. In the latter respect the behavior of the auroral oval consistently follows the pattern first described by WYAH75.

## 5. Discussion

**Further characterization of the nightside precipitation.** The scheme outlined herein does not exhaust the useful characterization of nightside precipitation. Some notable omissions are the existence of flux depletion regions, surge forms, and velocity-dispersed ion structures (VDIS-2) at the poleward edge of the oval.



**Figure 2.** The correlation coefficient of each spectrum with its neighboring predecessors for the pass shown in Plate 4. The dashed line illustrates b4s.

The identification of VDIS-2 events is of interest because it has been plausibly argued that such instances occur on field lines mapping to the high-altitude PSBL [Zelevni *et al.*, 1990], although observations of VDIS events seem to be a sufficient but not a necessary condition for making such a mapping [Burke *et al.*, 1994]. VDIS-2 structures are to be found between boundaries 5 and 6 when they are present. An example in the DMSP data set can be seen in Plate 1 of Senior *et al.* [1994]. As yet the criteria for identifying a structure as VDIS-2 are quite vague; it is not an easy thing to look at a spectrogram and infer that the ions exhibit a dispersion due to a velocity filter effect. We believe legitimate VDIS-2 signatures exist, but this matter needs careful consideration before code is introduced to automate their identification.

Flux depletion regions are characterized by deep drops in both electron and ion flux levels well within the auroral oval. These are distinguished from the drop-off in ion flux associated with the potential drops that accelerate electrons downward. An example of the latter phenomenon can be seen in Plate 3; an example of the former can be seen in Plate 14 of Sánchez *et al.* [1993]. It is believed that flux depletion regions correspond to rarefactions in the magnetotail.

Plate 3 also serves to illustrate an auroral bulge associated with the substorm expansion phase (note that ions are retarded from precipitating in the bulge). The distinctive structure of such an expansion bulge is a fairly constant downward-accelerating potential over a large spatial scale (as opposed to the rise and fall of inverted V-shaped structures). The scale of bulge forms (up to several hundred kilometers) is larger than typical of inverted V structures, although the latter can occasionally be of comparable scale. Because of their ease in identification and importance in substorm phenomenology, these events can also be included in the automated monitoring of the nightside magnetosphere.

**Discrete and diffuse aurora.** “Discrete” and “diffuse” aurora are terms thought to be universally understood but

which actually mean quite different things to different people. One minor point is that Lui *et al.* [1977] defined the diffuse aurora as a region exceeding 1 kR in intensity, whereas FG85 defined the diffuse aurora as a “subvisual” region at the equatorward edge of the aurora. This latter definition was given partly because relatively homogeneous emissions are difficult to resolve from ground-based observations (“subvisual” in the sense of being “unresolvable”), and partly because the actual intensity of the diffuse aurora is in dispute. The disagreement stems from differing definitions of the term “diffuse aurora.”

FG85, in keeping with Feldstein and Starkov [1967], identify the “oval of discrete auroral forms” as beginning when the first auroral arc occurs and extending to the poleward edge of the main oval. All precipitation between b3a and b5 (or perhaps b2t and b5) is part of the “discrete auroral oval.” This terminology is perfectly reasonable and widely used; however, one must then remember that what FG85 term the discrete auroral oval may include portions of what many satellite researchers separate out as the diffuse aurora (including all precipitation between b2e and b4s). Most individual spectra within this latter region do not exhibit signs of field-aligned electron acceleration or, indeed, any spatial structure on a scale 5–10 km or greater (i.e., each spectrum is highly correlated with its neighbors).

Qualitatively similar results have been obtained by Elphinstone *et al.* [1995] using simultaneous particle and imager observations. They report that, for the particular case they were studying, “the region of unstructured 1 to 10 keV electron precipitation overlaps with the main UV auroral oval.” This implies that the diffuse aurora is intense and energetic, as originally introduced by Lui *et al.* [1973]. Elphinstone *et al.* [1995] also agree that discrete auroral features can appear well inside the “CPS” region as traditionally defined. Likewise, an examination of Plate 2 of Lopez *et al.* [1991] shows an inverted V structure (at 0302:20 UT) deep within the region they identify as diffuse aurora—and reasonably so, since it is within the  $dE_e/d\lambda > 0$  region. Therefore under the Feldstein and Starkov [1967] definition, the region of diffuse aurora from satellite observations is in this case actually part of the oval of discrete forms. As a final example, Samson *et al.* [1992] have combined ground-based and satellite measurements to show that a discrete arc can appear deep within an originally unstructured precipitation region (the satellite CPS).

This difference in how the term diffuse aurora is defined explains why, according to FG85, nearly all of the precipitating energy flux into the ionosphere occurs in the oval of discrete forms, whereas to many satellite researchers significant energy flux into the ionosphere is deposited in the diffuse portion of the auroral oval.

We believe that both the Feldstein and Starkov [1967] definition of the oval of discrete forms and the satellite-based definition of spatially structured/unstructured precipitation are valid, but it is now clear that these definitions only approximately coincide. Moreover, it is known that auroral arcs as observed from the ground are narrower than can be resolved from most satellite observations. In fact the scale of auroral arcs is too small to reflect any magnetospheric structure [Borovsky, 1993]. Because the arcs tend to cluster into larger-scale groupings, in most cases a good relationship probably exists between the

large-scale electron acceleration events (5 to several hundred kilometers) observed by satellite and the very small-scale discrete arcs (tens or hundreds of meters) observed from the ground.

However, to promote precision and avoid apparent contradictions, we suggest limiting the terminology used according to the measurements made. The term “auroral arcs” is best reserved for use by ground-based researchers, or at least by those with the resolution capability to identify  $\sim 100$ -m structures (and to determine that the structure is extended in longitude). The satellite community can instead employ the terms “electron acceleration events,” “structured aurora,” and “unstructured aurora.” The first term is quantifiable by the presence of a monoenergetic peak or at least a sharp cutoff above the electron spectral peak. The structure or lack thereof can be determined by the correlation coefficient of individual spectra with their neighbors. Regions lacking accelerated electrons and for which each spectrum closely resembles its neighbors (correlation coefficient 0.6–0.95) are thus the regions of unstructured aurora. Note that not all structured aurora need show signs of electron acceleration.

Finally, the term “diffuse” aurora was introduced by *Lui and Anger* [1973] in the context of satellite imagery. Since the spatial resolution of such imagery is generally comparable to (or somewhat below) satellite particle data, it is likely that the diffuse aurora generally corresponds to the region of unstructured particle precipitation. However, this is not universally the case, because it is possible to have accelerated electrons with a fairly constant potential drop in auroral bulge features associated with the substorm expansion phase. Thus *Bythrow and Potemra* [1987] identify a large part of a DMSP optical auroral image as diffuse aurora, although an examination of the particle data shows that the electrons evince clear monoenergetic peaks throughout the region of bright emissions. Because only spatial structure and not acceleration features can be inferred from the imager, it is occasionally possible for a diffuse aurora to be “structured” in the spectral but not the spatial sense. This phenomenon is comparatively rare, however.

## 6. Summary and Conclusions

In this paper we have proposed a revised phenomenology of nightside precipitation including boundaries intended to facilitate the abstraction of geophysically significant information. We introduced specific quantitative algorithms to identify these boundaries in order to minimize operational ambiguity. Quantitative details are given in section 3, and justification (including appropriate references) is given in sections 2 and 4. A compact summary follows.

**Boundaries b1e,b1i.** The geophysical significance of these boundaries is that zero-energy particles experience no curvature or gradient drifts; hence, their earthward extent is determined solely by  $\mathbf{ExB}$  drifts. The zero-energy electron boundary often coincides with the plasmopause.

**Boundaries b2e,b2i,b2t.** In the equatorward portion of the auroral precipitation,  $dE_e/d\lambda > 0$ ; in the poleward portion,  $dE_e/d\lambda < 0$ . The point where  $dE_e/d\lambda = 0$  is termed b2e. One interpretation is that b2e is the start of the main plasma sheet. A boundary often located nearby is the  $>3$ -

keV ion-precipitating energy-flux maximum, which always occurs near the equatorward edge of the oval, just before the high-energy ion population becomes trapped. The ion isotropy poleward of b2i results from scattering in the current sheet where the gyroradius is comparable to the magnetic field line curvature; hence, b2i is a proxy for the current sheet earthward edge. A closely related boundary is the outer boundary of the Van Allen radiation belt, defined as the stable trapping boundary of  $>30$ – $40$ -keV electrons (b2t). This also is physically determined by scattering in the magnetotail current sheet.

**Boundaries b3a,b3b.** The most equatorward and poleward electron spectra which show signs of field-aligned acceleration through a potential drop (monoenergetic peaks) are termed boundaries b3a and b3b.

**Boundary b4s.** Electron precipitation near and sometimes poleward of boundary 2 often lacks spatial structure on a scale length of 5–10 km or larger, in the sense that each spectrum correlates highly with its neighbors (correlation coefficients in the range 0.6–0.95). Farther poleward, the electrons are more highly structured, with correlation coefficients between neighboring spectra generally in the 0.0–0.4 range. The dividing point between structured and unstructured electron precipitation is boundary b4s.

**Boundaries b5e,b5i.** The contiguous oval generally has a sharp poleward cutoff, with a drop in fluxes by a factor of at least 4 over a  $\sim 0.2^\circ$  latitudinal range. Although the cutoff is sharper for southward than northward IMF, even in the latter case the drizzle poleward of the oval is typically an order of magnitude less than anything observed in the main oval. Thus a clear poleward boundary to the oval exists, even under northward IMF conditions.

**Boundary b6.** Under active conditions, boundary 5 usually represents the poleward boundary of precipitation, except for a very narrow “overhang” region of weak electron precipitation in the  $\sim 10$ -keV range. Often, especially under quiet or quieting conditions, there is a region of low-energy electron and ion precipitation at low flux levels (1–3 orders of magnitude less intense than in the main oval), which is highly structured (in the sense of having neighboring spectra that are poorly correlated). The precipitation between b5 and b6 is termed the subvisual drizzle poleward of the oval. Boundary b6 is defined as the point where fluxes either drop to levels not easily measurable or drop until a polar rain signature is encountered.

The terms diffuse aurora, discrete aurora, auroral arcs, and electron acceleration events are being used in the literature in ways that, under some conditions, can lead to apparent contradictions. The ground-based “auroral oval of discrete forms” sometimes includes part of the region considered to be diffuse aurora from satellite observations. We recommend that the term auroral arcs be limited to use when instrumentation of resolution  $\sim 100$  m or better is available. Particle observations can identify an “unstructured” aurora, a term we have quantified as a region wherein the correlation coefficient of each individual spectrum with its neighbors lies in the 0.6–0.95 range. “Structured” particle observations are then those with a correlation coefficient below 0.6 (generally in the range 0.0–0.4). Such structure can be caused by field-aligned electron acceleration, but not all structured spectra show such signs. Finally, the term diffuse aurora originally referred to satellite imagery in which spatial structure was not identifiable.

It is reasonable to restore this original definition, taking note that a lack of spatial structure in an image usually, but not always, implies a lack of spectral structure in the corresponding precipitation.

**Acknowledgments.** We have benefited from discussions with L. A. Weiss, A. T. Y. Lui, K. Makita, and especially V. Sergeev. Work at APL was supported by AFOSR grant F49620-92-J-0196. Y. I. Feldstein acknowledges ISF grant M6P300, and Y. I. Galperin acknowledges RFFR grant 94-02-04299a. The DMSP SSJ4 instrument was designed and built by D. Hardy of the Phillips Laboratory.

The editor thanks J. D. Winningham and E. M. Basinska-Lewin for their assistance in evaluating this paper.

## References

- Baumjohann, W., G. Paschmann, and C. A. Cattell, Average plasma properties in the central plasma sheet, *J. Geophys. Res.*, **94**, 6597, 1989.
- Bernstein, W., B. Hultqvist, and H. Borg, Some implications of low altitude observations of isotropic precipitation of ring current protons beyond the plasmopause, *Planet. Space Sci.*, **22**, 767, 1974.
- Borovsky, J. E., Auroral arc thicknesses as predicted by various theories, *J. Geophys. Res.*, **98**, 6101, 1993.
- Bosqued, J. M., J. A. Sauvaud, and D. Delcourt, Precipitation of superthermal ionospheric ions accelerated in the conjugate hemisphere, *J. Geophys. Res.*, **91**, 7006, 1986.
- Burch, J. L., Low-energy electron fluxes at latitudes above the auroral zone, *J. Geophys. Res.*, **73**, 3585, 1968.
- Burke, W. J., J. S. Machuzak, N. C. Maynard, E. M. Basinska, G. M. Erickson, R. A. Hoffman, J. A. Slavin, and W. B. Hanson, Auroral ionospheric signatures of the plasma sheet boundary layer in the evening sector, *J. Geophys. Res.*, **99**, 2489, 1994.
- Bythrow, P. F., and T. A. Potemra, Birkeland currents and energetic particles associated with optical auroral signatures of a westward traveling surge, *J. Geophys. Res.*, **92**, 8691, 1987.
- Cambou, F., and Y. I. Galperin, Overall results from the ARCAD experiment aboard the satellite AUREOLE, in *International Symposium on Solar-Terrestrial Physics*, p. 396, Sao Paulo, Brazil, 1974.
- Cambou, F., and Y. I. Galperin, Main results of the joint French-Soviet space project ARCAD-1 and ARCAD-2 for magnetospheric, auroral and ionospheric physics, *Ann. Geophys.*, **38**, 87, 1982.
- Christon, S. P., D. J. Williams, D. G. Mitchell, L. A. Frank, and C. Y. Huang, Spectral characteristics of plasma sheet ion and electron populations during undisturbed geomagnetic conditions, *J. Geophys. Res.*, **94**, 13,409, 1989.
- Deehr, C. S., J. D. Winningham, F. Yasuhara, and S.-I. Akasofu, Simultaneous observations of discrete and diffuse auroras by the Isis 2 satellite and airborne instruments, *J. Geophys. Res.*, **81**, 5527, 1976.
- Eastman, T. E., L. A. Frank, W. K. Peterson, and W. Lennartsson, The plasma sheet boundary layer, *J. Geophys. Res.*, **89**, 1553, 1984.
- Eather, R. H., Latitudinal distributions of auroral and airglow emissions: The "soft" auroral zone, *J. Geophys. Res.*, **74**, 153, 1969.
- Elphinstone, R. D., et al., The double oval UV auroral distribution, 1, Implications for the mapping of auroral arcs, *J. Geophys. Res.*, **100**, 12,075, 1995.
- Fairfield, D. H., and A. F. Vinas, The inner edge of the plasma sheet and the diffuse aurora, *J. Geophys. Res.*, **89**, 841, 1984.
- Feldstein, Y. I., and Y. I. Galperin, The auroral luminosity structure in the high-latitude upper atmosphere: Its dynamics and relationship to the large-scale structure of the Earth's magnetosphere, *Rev. Geophys.*, **23**, 217, 1985.
- Feldstein, Y. I., and G. V. Starkov, Dynamics of auroral belt and polar geomagnetic disturbances, *Planet. Space Sci.*, **15**, 209, 1967.
- Feldstein, Y. I., and G. V. Starkov, The auroral oval and the boundary of closed field lines of geomagnetic field, *Planet. Space Sci.*, **18**, 501, 1970.
- Frank, L. A., Plasma in the Earth's polar magnetosphere, *J. Geophys. Res.*, **76**, 5202, 1971.
- Frank, L. A., and K. L. Ackerson, Observations of charged particle precipitation into the auroral zone, *J. Geophys. Res.*, **76**, 3612, 1971.
- Galperin, Y. I., and Y. I. Feldstein, Auroral luminosity and its relationship to magnetospheric plasma domains, in *Auroral Physics*, edited by C.-I. Meng, M. J. Rycroft, and L. A. Frank, p. 207, Cambridge Univ. Press, New York, 1991.
- Galperin, Y. I., V. N. Ponomarev, Y. N. Ponomarev, and A. G. Zosimov, Plasma convection in the evening sector of the magnetosphere and the nature of the plasmopause (in Russian), *Cosmic Res.*, **13**, 669, 1975.
- Galperin, Y. I., N. V. Jorjio, R. A. Kovrazhkin, F. Cambou, J. A. Sauvaud, and J. Crasnier, On the origin of auroral protons at the day-side auroral oval, *Ann. Geophys.*, **32**, 117, 1976.
- Galperin, Y. I., J. Crasnier, Y. V. Lissakov, L. M. Nikolaenko, V. M. Sinitsin, J. A. Sauvaud, and V. L. Khalipov, Diffuse auroral zone, 1, Model of the equatorial boundary of diffuse auroral electron precipitation zone in the evening and near midnight sectors (in Russian), *Cosmic Res.*, **15**, 421, 1977.
- Galperin, Y. I., V. A. Gladyshev, N. V. Jorjio, R. A. Kovrazhkin, V. M. Sinitsin, F. Cambou, J. A. Sauvaud, and J. Crasnier, Adiabatic acceleration induced by convection in the plasma sheet, *J. Geophys. Res.*, **83**, 2567, 1978.
- Hardy, D. A., L. K. Schmitt, M. S. Gussenhoven, F. J. Marshall, H. C. Yeh, T. L. Shumaker, A. Hube, and J. Pantazis, Precipitating electron and ion detectors (SSJ/4) for the block 5D/flights 6-10 DMSP satellites: Calibration and data presentation, *Rep. AFGL-TR-84-0317*, Air Force Geophys. Lab., Hanscom Air Force Base, Mass., 1984.
- Heikkila, W. J., and J. D. Winningham, Penetration of magnetosheath plasma to low altitudes through the dayside magnetospheric cusps, *J. Geophys. Res.*, **76**, 883, 1971.
- Horwitz, J. L., S. Menteer, J. Turnley, J. L. Burch, J. D. Winningham, C. R. Chappell, J. D. Craven, L. A. Frank, and D. W. Slater, Plasma boundaries in the inner magnetosphere, *J. Geophys. Res.*, **91**, 8861, 1986.
- Johnson, R. G., R. D. Sharp, M. F. Shea, and G. B. Shook, Satellite observations of two distinct dayside zones of auroral electron precipitation (abstract), *Eos Trans. AGU*, **47**, 64, 1966.
- Jorjio, N. V., J. Crasnier, J. A. Sauvaud, and V. M. Sinitsin, Auroral diffuse zone, III, Comparison between the equatorial border of the diffuse auroral zone and the plasmopause position during February 13 and 17, 1972 magnetic storms (in Russian), *Cosmic Res.*, **16**, 937, 1978.
- Jorjio, N. V., R. A. Kovrazhkin, M. M. Mogilevsky, J. M. Bosqued, H. Reme, J. A. Sauvaud, C. Beghin, and J. L. Rauch, Detection of suprathermal ionospheric O<sup>+</sup> ions inside the plasmasphere, *Adv. Space Res.*, **141**, 1985.
- Konradi, A., C. L. Semar, and T. A. Fritz, Substorm-injected protons and electrons and the injection boundary model, *J. Geophys. Res.*, **80**, 3055, 1975.
- Lassen, K., J. R. Sharber, and J. D. Winningham, The development of auroral and geomagnetic substorm activity after

- a southward turning of the interplanetary magnetic field following several hours of magnetic calm, *J. Geophys. Res.*, **82**, 5031, 1977.
- Lopez, R. E., H. E. Spence, and C.-I. Meng, DMSP F7 observations of a substorm field-aligned current, *J. Geophys. Res.*, **96**, 19,409, 1991.
- Lui, A. T. Y., and C. D. Anger, A uniform belt of diffuse auroral emission seen by the Isis-2 scanning photometer, *Planet. Space Sci.*, **21**, 809, 1973.
- Lui, A. T. Y., D. Venkatesan, C. D. Anger, S.-I. Akasofu, W. J. Heikkila, J. D. Winningham, and J. R. Burrows, Simultaneous observations of particle precipitations and auroral emissions by the ISIS 2 satellite in the 19-24 MLT sector, *J. Geophys. Res.*, **82**, 2210, 1977.
- Lui, A. T. Y., R. W. McEntire, and S. M. Krimigis, Evolution of the ring current during two geomagnetic storms, *J. Geophys. Res.*, **92**, 7459, 1987.
- Lyons, L. R., and T. W. Speiser, Evidence for current sheet acceleration in the geomagnetic tail, *J. Geophys. Res.*, **87**, 2276, 1982.
- Lyons, L. R., J. F. Fennell, and A. L. Vampola, A general association between discrete auroras and ion precipitation from the tail, *J. Geophys. Res.*, **93**, 12,932, 1988.
- Mauk, B. H., and C.-I. Meng, Dynamical injections as the source of near geostationary quiet time particle spatial boundaries, *J. Geophys. Res.*, **88**, 100,011, 1983.
- Newell, P. T., and C.-I. Meng, Energy dependence of the equatorward cutoffs in auroral electron and ion precipitation, *J. Geophys. Res.*, **92**, 7519, 1987.
- Newell, P. T., and C.-I. Meng, The cusp and the cleft/boundary layer: Low altitude identification and statistical local time variation, *J. Geophys. Res.*, **93**, 14,549, 1988a.
- Newell, P. T., and C.-I. Meng, Categorization of dispersion curves in the equatorward edge of the diffuse aurora, *Planet. Space Sci.*, **36**, 1031, 1988b.
- Newell, P. T., W. J. Burke, C.-I. Meng, E. R. Sánchez, and M. E. Greenspan, Identification of the plasma mantle at low altitude, *J. Geophys. Res.*, **96**, 35, 1991a.
- Newell, P. T., W. J. Burke, E. R. Sánchez, C.-I. Meng, M. E. Greenspan, and C. R. Clauer, The low-altitude boundary layer and the boundary plasma sheet at low altitude: Prenoon precipitation regions and convection reversal boundaries, *J. Geophys. Res.*, **96**, 21,013, 1991b.
- Newell, P. T., S. Wing, C.-I. Meng, and V. Sigillito, The auroral oval position, structure, and intensity of precipitation from 1984 onward: An automated online data base, *J. Geophys. Res.*, **96**, 5877, 1991c.
- Newell, P. T., K. M. Lyons, and C.-I. Meng, A large survey of electron acceleration events, *J. Geophys. Res.*, **101**, in press, 1996.
- Nishida, A., Formation of plasmopause, or magnetospheric plasma knee, by the combined action of magnetosphere convection and plasma escape from the tail, *J. Geophys. Res.*, **71**, 5669, 1966.
- Rostoker, G., and T. Eastman, A boundary layer model for magnetospheric substorms, *J. Geophys. Res.*, **92**, 12,187, 1987.
- Samson, J. C., L. R. Lyons, P. T. Newell, F. Creutzberg, and B. Xu, Proton aurora and substorm intensifications, *Geophys. Res. Lett.*, **19**, 2167, 1992.
- Sánchez, E. R., B. H. Mauk, P. T. Newell, and C.-I. Meng, Low-altitude observations of the evolution of substorm injection boundaries, *J. Geophys. Res.*, **98**, 5815, 1993.
- Sauvaud, J. A., Y. I. Galperin, V. A. Gladyshev, A. K. Kuzmin, T. M. Muliarchick, and J. Crasnier, Spatial inhomogeneity of magnetosheath proton precipitation along the dayside cusp from the ARCAD experiment, *J. Geophys. Res.*, **85**, 5105, 1980.
- Sauvaud, J. A., J. Crasnier, K. Moula, R. A. Kovrazhkin, and N. V. Jorjio, Morning sector ion precipitation following substorm injections, *J. Geophys. Res.*, **86**, 3430, 1981.
- Sauvaud, J. A., J. Crasnier, Y. I. Galperin, and Y. I. Feldstein, A statistical study of the dynamics of the equatorial boundary of the diffuse aurora in the pre-midnight sector, *Geophys. Res. Lett.*, **10**, 749, 1983.
- Schild, M. A., and L. A. Frank, Electron observations between the inner edge of the plasma sheet and the plasmasphere, *J. Geophys. Res.*, **75**, 5401, 1970.
- Senior, C., D. C. Delcourt, J. C. Cerisier, C. Hanuise, J. P. Villain, R. G. Greenwald, P. T. Newell, and F. J. Rich, Correlated observations of the boundary between polar cap and nightside auroral zone by HF radars and the DMSP satellite, *Geophys. Res. Lett.*, **21**, 221, 1994.
- Sergeev, V. A., and B. B. Gvozdevsky, MT-index, A possible new index to characterize magnetic configuration of magnetotail, *Ann. Geophys.*, **13**, 1093, 1995.
- Sergeev, V. A., E. M. Sazhina, N. A. Tsyganenko, J. A. Lundblad, and F. Soraas, Pitch-angle scattering of energetic protons in the magnetotail current sheet as the dominant source of their isotropic precipitation into the nightside ionosphere, *Planet. Space Sci.*, **31**, 1147, 1983.
- Sergeev, V. A., M. Malkov, and K. Mursula, Testing the isotropic boundary algorithm method to evaluate the magnetic field configuration in the tail, *J. Geophys. Res.*, **98**, 7609, 1993.
- Vasyliunas, V. M., A survey of low-energy electrons in the evening sector of the magnetosphere with OGO 1 and OGO 3, *J. Geophys. Res.*, **73**, 2839, 1968.
- Weiss, L. A., P. H. Reiff, R. V. Hilmer, J. D. Winningham, and G. Lu, Mapping the auroral oval into the magnetotail using Dynamics Explorer plasma data, *J. Geomagn. Geoelectr.*, **44**, 1121, 1992.
- Winningham, J. D., F. Yasuhara, S.-I. Akasofu, and W. J. Heikkila, The latitudinal morphology of 10-eV to 10-keV electron fluxes during magnetically quiet and disturbed times in the 2100-0300 MLT sector, *J. Geophys. Res.*, **80**, 3148, 1975.
- Zelenyi, L., R. Kovrazhkin, and J. M. Bosqued, Velocity-dispersed ion beams in the nightside auroral zone: Aureole m3 observations, *J. Geophys. Res.*, **95**, 12,119, 1990.

Y. I. Feldstein, Institute of Terrestrial Magnetism, Ionosphere and Radiowave Propagation, Troitsk, Russia. (e-mail: gromova@charley.izmiyan.rssi.ru)

Y. I. Galperin, Institute of Space Research of the Academy of Sciences of Russia, Moscow, Russia. (e-mail: YGALPERIN@romance.iki.rssi.ru)

C.-I. Meng and P. T. Newell, Johns Hopkins University, Applied Physics Laboratory, Johns Hopkins Road, Laurel, MD 20723-6099. (e-mail: patrick.newell@jhuapl.edu)

(Received April 27, 1995; revised September 14, 1995; accepted November 15, 1995.)